Journal of Rare Earths 36 (2018) 142–147

Contents lists available at ScienceDirect

Journal of Rare Earths

journal homepage: http://www.journals.elsevier.com/journal-of-rare-earths

Active manganese oxide on MnO_x–CeO_2 catalysts for low-temperature NO oxidation: Characterization and kinetics study☆

Lingkun Meng [a], Jun Wang [a], Zhihui Sun [a], Jinxin Zhu [a], Hang Li [a], Jianqiang Wang [a], Meiqing Shen [a, b, c, *]

[a] *Key Laboratory for Green Chemical Technology of State Education Ministry, School of Chemical Engineering & Technology, Tianjin University, Tianjin 300072, China*
[b] *Collaborative Innovation Centre of Chemistry Science and Engineering (Tianjin), Tianjin 300072, China*
[c] *State Key Laboratory of Engines, Tianjin University, Tianjin 300072, China*

ARTICLE INFO

Article history:
Received 11 April 2017
Received in revised form
27 May 2017
Accepted 31 May 2017
Available online 25 August 2017

Keywords:
MnO_x–CeO_2
NO oxidation
Active manganese oxide
Reaction kinetics
Rare earths

ABSTRACT

MnO_x–CeO_2 catalysts were synthesized to investigate the active sites for NO oxidation by varying the calcination temperature. XRD and TEM results showed that cubic CeO_2 and amorphous MnO_x existed in MnO_x–CeO_2 catalysts. High temperature calcination caused the sintering of amorphous MnO_x and transforming to bulk crystalline Mn_2O_3. H_2-TPR and XPS results suggested the valence of Mn in MnO_x–CeO_2 was higher than pure MnO_x, and decreased with the increasing calcination temperature. The turnover frequency (TOF) was calculated based on the initial reducibility according to H_2-TPR quantitation and kinetic study. The TOF results indicated that the initial reducibility of amorphous MnO_x with high valence manganese ions was equivalent to the active sites for NO oxidation. It can be inferred that the amorphous MnO_x plays a key role in low-temperature NO oxidation.

NO_x deriving from diesel engines remains a major source of air pollution. To meet the criteria of changing stringent emission limits, engineers and catalysts researchers, are endeavoring to develop more efficient de-NO_x techniques. Two typical techniques, NSR (NO_x storage and reduction) and SCR (selective catalytic reduction), have been developed to convert NO_x to harmless N_2. In both techniques, NO to NO_2 oxidation reaction is a critical step. During the lean period in NSR, NO needs to be oxidized to NO_2. NO_2 is easier to adsorbed on the storage components and promote the NO_x trapping capacity, which further enhances the fuel-economy and de-NO_x efficiency.[1,2] Analogically, in SCR technique, NO_2 is considered to inspire fast SCR reaction.[3] These two techniques are mostly applied in the downstream of diesel oxidation catalyst (DOC), oxidizing NO to NO_2. Besides, the soot can be oxidized by NO_2 to achieve the passive regeneration of diesel particulate filter (DPF).[4] The catalysts for NO oxidation to NO_2 take a key role in exhaust after-treatment systems. Therefore, many research groups have devoted to developing high-performance NO oxidation catalysts.

Pt-based catalysts have excellent catalytic oxidation activity, and have long been used for NO oxidation to NO_2.[5] Liu et al[6] reported that the acidic H-ZSM5 support promoted the preferential adsorption of NO_2 on the surface of soot and the surface strong acid sites might catalyze the formation and decomposition of surface oxygenated complexes on soot. Villani et al[7] investigated the effects of Pt particle size and support on the NO oxidation activity over Pt catalysts. It has been reported that DOC accounts for a large part of platinum in the noble metal market.[8] However, its application is limited to the high cost of noble metals. Thus, the inexpensive NO oxidation catalysts with high catalytic performance are required to develop to substitute noble metal catalysts.

In recent years, inexpensive MnO_x–CeO_2 oxides have attracted growing attentions since the catalysts show remarkable activity in oxidizing CO,[9] CH_x[10] and VOC compounds.[11,12] Yang et al[13] reported the catalytic NO oxidation performance over MnO_x–CeO_2 in NH_3-SCR reaction. Several researchers have studied the synergistic effect between MnO_x and CeO_2, as well as the active sites of NO

☆ **Foundation item**: Project supported by the National key research and development program (2016YFC0204901), the National Natural Science Foundation of China (21576207) and the introduction of talent and technology cooperation plan of Tianjin (14RCGFGX00849).

* Corresponding author. Key Laboratory for Green Chemical Technology of State Education Ministry, School of Chemical Engineering & Technology, Tianjin University, Tianjin 300072, China.

E-mail address: mqshen@tju.edu.cn (M.Q. Shen).

http://dx.doi.org/10.1016/j.jre.2017.05.017

oxidation reaction over MnO_x–CeO_2 catalyst. Wu et al[14] considered the synergistic effect between MnO and CeO_2 as a process of oxygen activation, and the oxygen transferred through the redox recycles of Mn^{4+}/Mn^{3+} and Ce^{4+}/Ce^{3+}. Qi et al[15] emphasized the significance of the active oxygen species generated through the vacancy on the interface between Ce and Mn. However, so far, the active sites are still controversial and remain to be explored.

Our previous work[16] reported that the Mn^{4+} and the activated oxygen were favorable for NO oxidation reaction, but had no direct evidence about the active sites. It has been reported that the calcination temperature can affect the structure and valence of MnO_x,[17,18] which further influence the reaction activity. Based on the previous work and the effects of calcination temperature on the catalysts, the active sites for NO oxidation over MnO_x–CeO_2 were studied. In this work, we investigated the NO oxidation over the MnO_x–CeO_2 calcined at different temperatures, pure MnO_x and CeO_2 samples. The structure features, oxidation states, and redox properties of these catalysts were characterized by XRD, HR-TEM, XPS and H_2-TPR. The active sites for NO oxidation of MnO_x–CeO_2 catalysts were proposed based on the kinetics study and H_2-TPR results.

1. Experimental

1.1. Sample synthesis

The samples were prepared by the co-precipitation method. $Mn(NO_3)_2$ and $Ce(NO_3)_3 \cdot 6H_2O$ with a Mn/(Mn + Ce) mole ratio of 0.4 were dissolved to make a solution (1 mol/L). Then the solution along with H_2O_2 was added to $NH_3 \cdot H_2O$ with stirring at room temperature. The amount of aqueous ammonia solution was 100% excess compared to the reaction stoichiometry. Lastly, PEG2000 was introduced to the mixture. The crystallization process of the obtained suspension was conducted at 70 °C in the mother liquid for 12 h. Then the mixture was filtered, washed, and dried at 90 °C overnight. The dried precursor was calcined at 550, 650, and 750 °C under the flow of air for 5 h, denoted as MC-550, MC-650 and MC-750, respectively. For comparison experiments, pure CeO_2 and MnO_x were prepared in the same procedure with a calcination temperature of 550 °C, denoted as C-550 and M-550, respectively.

1.2. Characterization

The structure of the catalysts was identified by X-ray diffraction (XRD) on an X'Pert Pro diffractometer using Cu Kα ($\lambda = 0.15418$ nm) with a power of 40 kV × 40 mA. The data from 2θ range of 20°–90° were collected with the step size of 0.02°.

Specific surface areas were tested on F-sorb 3400 volumetric adsorption/desorption apparatus at liquid nitrogen temperature using the BET model. Prior to the tests, the samples were pretreated under vacuum at 150 °C for 3 h.

High resolution transmission electron microscopy (HR-TEM) and Energy dispersive X-Ray spectroscopy (EDS) experiments of M-550 were conducted with transmission Tecnai G2 F20 equipped with a Gatan imaging filter operated at 200 kV.

X-ray photoelectron spectroscopy (XPS) experiments were conducted with a PHI-1600 ESCA spectrometer with a non-monochromatic Mg Kα ($h\nu = 1253.6$ eV) radiation source operating at 15 kV and 400 W. The background pressure in the XPS chamber was kept below 0.67×10^{-6} Pa. The binding energy (BE) was calibrated based on the line position of C 1s (284.6 eV).

H_2-TPR measurement was performed in a U-type reactor with 100 mg sample. The sample was firstly pretreated in 5% O_2/N_2 at 300 °C for 30 min, then cooled down to room temperature with N_2 purging. Then the 5% H_2/N_2 was introduced with a flow rate of 30 mL/min. The sample was heated up from room temperature to 900 °C at 10 °C/min. The temperature programmed reduction profile during the reduction was measured by a thermal conductivity detector (TCD).

1.3. Activity evaluation

Catalytic activity tests for NO oxidation were carried out in a quartz tubular reactor. 0.2 g of catalyst sample (60–80 mesh) and 0.8 g of quartz sand (60–80 mesh) were packed and sandwiched between two quartz wool plug. Prior to the test, the catalysts were pretreated in 10% O_2 at 500 °C for 1 h. The feed gas contained 100 ppm NO, 10% O_2, 5% CO_2, 5% H_2O and balanced by N_2 with 850 mL/min total flow (GHSV = 30,000 h^{-1}), the outlet gas was analyzed by FT-IR spectrometer (MKS 2030). The activity tests were conducted at temperatures from 150 to 450 °C at an interval of 50 °C. The steady-state NO conversion was calculated according to the following equation:

$$\text{NO conversion} = \frac{[\text{NO}]_{\text{inlet}} - [\text{NO}]_{\text{outlet}}}{[\text{NO}]_{\text{inlet}}} \times 100\% \tag{1}$$

$[\text{NO}]_{\text{inlet}}$ is the inlet concentration of NO; $[\text{NO}]_{\text{outlet}}$ is the outlet concentration of NO.

NO oxidation to NO_2 is an exothermic reversible reaction which is limited by the thermodynamic equilibrium at higher temperatures. The equilibrium curve is calculated by the Van't Hoff equation:

$$\frac{\mathrm{dln}K_p}{\mathrm{d}T} = \frac{\Delta H(T)}{RT^2} \tag{2}$$

$$K_\mathrm{p} = \frac{p_{NO_2}}{p_{NO} \cdot p_{O_2}^{1/2}} \tag{3}$$

K_p, ΔH, R, T, p_{NO}, p_{O_2}, and p_{NO_2} represent equilibrium constant, reaction enthalpy, gas constant, reaction temperature, the partial pressures of NO, O_2 and NO_2, respectively.[19]

2. Results and discussion

2.1. Catalytic activity

Fig. 1 shows the results of NO oxidation over C-550, M-550 and MC samples. The NO conversion increases with the increasing

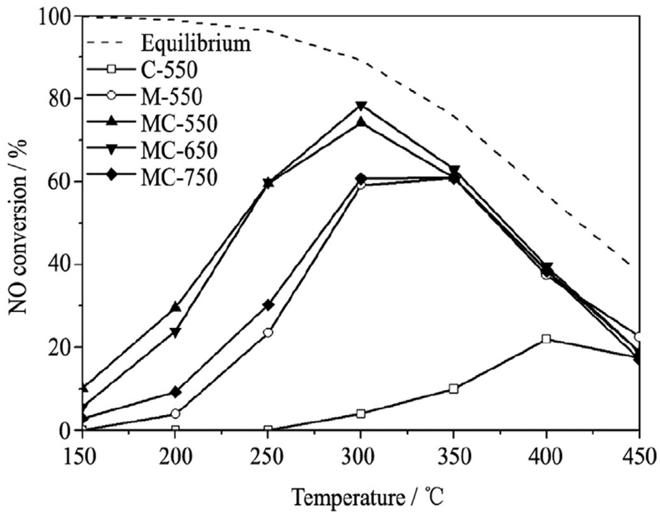

Fig. 1. NO conversion curves of C-550, M-550 and MC samples.